Magnetic domain structures of ferromagnetic ultra-thin films deposited on superconducting substrates

1997 J. Phys.: Condens. Matter 9 1019

(http://iopscience.iop.org/0953-8984/9/5/008)

J. Phys.: Condens. Matter **9** (1997) 1019–1030. Printed in the UK PII: S0953-8984(97)77806-8

Magnetic domain structures of ferromagnetic ultra-thin films deposited on superconducting substrates

A Stankiewicz†‡, S J Robinson‡, G A Gehring‡§ and V V Tarasenko†

† Institute of Physics, Warsaw University Branch, 41 Lipowa Street, 15-424 Bialystok, Poland
‡ Department of Physics, University of Sheffield, The Hicks Building, Sheffield S3 7RH, UK

Received 2 August 1996

Abstract. The influence of bulk superconducting substrates and coatings on the domain structure parameters of a ferromagnetic ultra-thin film was analysed, assuming the validity of the London equation in the superconducting volumes. The problem was analysed for both easy plane and perpendicular easy axis films; however, as the effects of the superconducting substrate are relatively unimportant for films magnetized in plane, most of the article is devoted to easy axis films. Expressions for the demagnetization energy were found for arbitrary magnetization distribution. It was shown that a superconducting substrate changes the domain structure properties even if the layer is coated with a non-superconducting material. For sufficiently thin films the domain structure can be fully suppressed, which was shown by considering an isolated Bloch wall for larger anisotropy ($Q > 1$) and the critical domain structure for low anisotropy ($Q < 1$). The results of numerical calculations for critical ferromagnetic film thickness (as a function of anisotropy and London penetration depth) are presented.

1. Introduction

Ultra-thin ferromagnetic films and multilayers have been attracting much interest recently, for both showing novel physical properties and giving new possibilities in applications [1]. This interest is also related to domain structures observed in these materials. The fast development of technology allows us to expect that new materials of this type will be available soon, including layers deposited on bulk superconducting substrates. Such combinations have already been investigated in a few publications, but only for superconducting surroundings on both sides. Reference [2] presents calculations of the critical domain structure, in the vicinity of the phase transition induced by an external in-plane field, showing that in sufficiently thin films there is a transition to a canted phase, rather than to a domain structure. There is a suggestion, supported by numerical comparison of the free energy in the monodomain state and domain structure, that the monodomain state can represent the minimum of energy even for a low in-plane field. The aim of the present work is to deal systematically with domain structure parameters in the absence of an in-plane field. Some analysis of this problem has been already performed in [3], but we are not able to confirm its conclusions in the appropriate limits.

As was shown in [4], the equilibrium domain structure of the infinite ultra-thin plate has the form of stripes, with finite size for any finite thickness. This size tends to infinity as the film thickness decreases to zero. Such an effect is related to the asymptotic

§ Corresponding author.

behaviour of the dipolar energy at small thickness. However, in the case of superconducting substrates the demagnetizing fields are created not only by the ferromagnet itself, but also by superconducting currents. For an ideal superconductor (characterized by a zero field penetration depth) the last contribution is equivalent to the mirror image of the ferromagnet. In the case of perpendicular magnetic moment, its image has the opposite direction (figure 1).

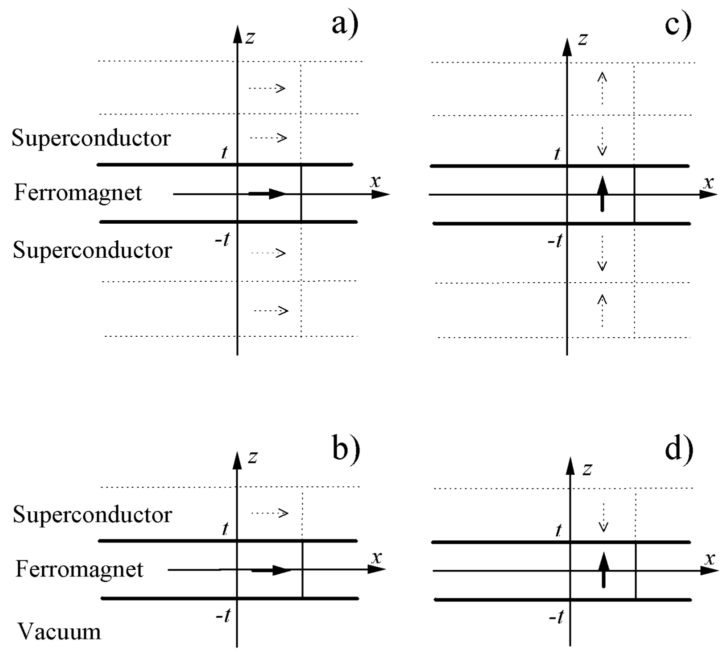

Figure 1. Magnetic moment inside the ferromagnetic film and its images inside ideal superconducting surroundings for easy plane (a, b) and easy axis (c, d). (a) and (c) correspond to the symmetric case, and (b) and (d) correspond to vacuum capping. The film is infinite in both the x and y directions.

In the case of in-plane anisotropy the image has the same direction as the original magnetic moment, so the superconducting substrate and normal capping combination doubles the effective thickness of the film (figure 1(b)). This corresponds to double demagnetizing energy, which can change an equilibrium domain size. At the same time the superconducting substrate–capping combination produces field distribution similar to that of the bulk material (figure 1(a)). However, in both cases the demagnetizing field is created mostly by the free poles on the film edges and the domain size is strongly dependent on the film in-plane size.

For perpendicular easy axis film the image has the opposite direction to the original moment (figure 1(c, d)). Hence, far away from its location, the field loses the dipolar characteristic and decrease much faster. It is clear that such behaviour of the demagnetization field can lead to new effects.

2. Basic equations

We will consider an infinite ferromagnetic film of thickness $2t$ bounded by planes $z = \pm t$. We start from the most general problem, assuming that half-spaces $z > t$ and $z < -t$ (figure 1) are filled with different superconducting materials, characterized by the penetration depths λ_+ and λ_- respectively.

2.1. A ferromagnet $|z| < t$

We assume that the field inside the ferromagnet $\boldsymbol{H}_F$ is described by Maxwell equations in the magnetostatic limit:

$$\begin{cases} \nabla \times \boldsymbol{H}_F = 0 \\ \nabla(\boldsymbol{H}_F + 4\pi \boldsymbol{M}) = 0 \end{cases} \tag{1}$$

which is equivalent to

$$\begin{cases} \boldsymbol{H}_F = \nabla \Phi \\ \nabla^2 \Phi = -4\pi \operatorname{div} \boldsymbol{M} \end{cases} \tag{2}$$

where $\boldsymbol{M}$ is the local magnetization vector and Φ represents the scalar potential.

In the very thin film (or at relatively large perpendicular anisotropy) the magnetization distribution along the z-axis can be treated as uniform inside the ferromagnet and the Fourier components of the potential Φ with respect to the sample plane can be found in the form

$$\Phi_{\boldsymbol{k}}(z) = A_{\boldsymbol{k}} \cosh kz + B_{\boldsymbol{k}} \sinh kz + (4\pi/k^2) \\ \times[\mathrm{i}(1 - \mathrm{e}^{-kt} \cosh kz)(\boldsymbol{k} \cdot \boldsymbol{M}_{\boldsymbol{k}}) - kM^z_{\boldsymbol{k}}\, \mathrm{e}^{-kt} \sinh kz]. \tag{3}$$

The related field components are given by

$$\begin{cases} \boldsymbol{H}^{\parallel}_{\boldsymbol{k}}(z) = \mathrm{i}\boldsymbol{k}\Phi_{\boldsymbol{k}}(z) \\ H^z_k(z) = \Phi'_{\boldsymbol{k}}(z). \end{cases} \tag{4}$$

2.2. A superconductor $|z| > t$

The first of the equations (1) is replaced by the London equation:

$$\begin{cases} \boldsymbol{H}_s + \lambda^2_{\pm} \nabla \times (\nabla \times \boldsymbol{H}_s) = 0 \\ \nabla \cdot \boldsymbol{H}_s = 0. \end{cases} \tag{5}$$

We neglect any vortex structure as is especially well justified for ultra-thin films, as their stray fields are very small. The solution of the equations (5) in terms of in-plane Fourier components can be expressed as

$$\boldsymbol{H}^{\pm}_{\boldsymbol{k}}(z) = \left(\mathrm{i}\boldsymbol{k}m \frac{k^2}{k_{\pm}} \boldsymbol{e}_z\right) \Phi^{\pm}_{\boldsymbol{k}} \exp k_+[(tmz)] \tag{6}$$

where $k^2_{\pm} = k^2 + \lambda^{-2}_{\pm}$ and $\boldsymbol{e}_z$ is the unit vector along the z-axis.

2.3. Boundary conditions

We will apply standard boundary conditions

$$\begin{cases} \boldsymbol{H}_{\boldsymbol{k}}^{\parallel}(\pm t) = \boldsymbol{H}_{\boldsymbol{k}}^{\parallel\pm}(\pm t) \\ H_{\boldsymbol{k}}^{z}(\pm t) + 4\pi M_{\boldsymbol{k}}^{z} = H_{\boldsymbol{k}}^{z\pm}(\pm t). \end{cases} \tag{7}$$

We will look for the solution, taking the scalar potential in the form

$$\Phi_{\boldsymbol{k}}^{\pm} = A_{\boldsymbol{k}} \cosh kt \pm B_{\boldsymbol{k}} \sinh kt + (2\pi/k^2)(1 - \mathrm{e}^{-2kt})(\mathrm{i}\boldsymbol{k} \cdot \boldsymbol{M}_{\boldsymbol{k}} m k M_{\boldsymbol{k}}^{z}). \tag{8}$$

Then the potential amplitudes are equal:

$$A_{\boldsymbol{k}} = \frac{4\pi(1 - \mathrm{e}^{-2kt})\,\mathrm{e}^{-kt}}{k^2[(1+\kappa_+)(1+\kappa_-) - (1-\kappa_+)(1-\kappa_-)\,\mathrm{e}^{-4kt}]} \times \{\mathrm{i}\boldsymbol{k}\cdot\boldsymbol{M}_{\boldsymbol{k}}[1 - \kappa_+\kappa_- + (1-\kappa_+)(1-\kappa_-)\,\mathrm{e}^{-2kt}] + kM_{\boldsymbol{k}}^{z}(\kappa_+ - \kappa_-)\} \tag{9a}$$

$$B_{\boldsymbol{k}} = \frac{4\pi(1 - \mathrm{e}^{-2kt})\,\mathrm{e}^{-kt}}{k^2[(1+\kappa_+)(1+\kappa_-) - (1-\kappa_+)(1-\kappa_-)\,\mathrm{e}^{-4kt}]} \times \{\mathrm{i}\boldsymbol{k}\cdot\boldsymbol{M}_{\boldsymbol{k}}(\kappa_+ - \kappa_-) + kM_{\boldsymbol{k}}^{z}[1 - \kappa_+\kappa_- - (1-\kappa_+)(1-\kappa_-)\,\mathrm{e}^{-2kt}]\} \tag{9b}$$

where

$$\kappa_\pm = k/k_\pm = k/\sqrt{k^2 + \lambda_\pm^{-2}}. \tag{10}$$

There are two particular cases, which are of special interest.

2.3.1. The symmetric configuration ($\lambda_+ = \lambda_-$).

In this case $A_{\boldsymbol{k}}$ and $B_{\boldsymbol{k}}$ simplify to the forms given below:

$$A_{\boldsymbol{k}} = \{4\pi(1-\kappa_+)(1-\mathrm{e}^{-2kt})\mathrm{e}^{-kt}/k^2[1+\kappa_+ - (1-\kappa_+)\mathrm{e}^{-2kt}]\}\mathrm{i}\boldsymbol{k}\cdot\boldsymbol{M}_{\boldsymbol{k}} \tag{11a}$$

$$B_{\boldsymbol{k}} = \{4\pi(1-\kappa_+)(1-\mathrm{e}^{-2kt})\mathrm{e}^{-kt}/k[1+\kappa_+ + (1-\kappa_+)\mathrm{e}^{-2kt}]\}\boldsymbol{M}_{\boldsymbol{k}}^{2}. \tag{11b}$$

2.3.2. Non-superconducting cover ($\lambda_- = \infty$).

In this limit $A_{\boldsymbol{k}}$ and $B_{\boldsymbol{k}}$ are given by

$$A_{\boldsymbol{k}} = B_{\boldsymbol{k}} = [2\pi(1-\kappa_+)(1 - \mathrm{e}^{-2kt})\mathrm{e}^{-kt}/k^2(1+\kappa_+)](\mathrm{i}\boldsymbol{k}\cdot\boldsymbol{M}_{\boldsymbol{k}} - kM_{\boldsymbol{k}}^{z}). \tag{12}$$

2.4. Demagnetization energy

The demagnetization energy E_d for the whole system (i.e. ferromagnet and superconductor) can be evaluated by direct integration over the whole space:

$$E_d = \frac{1}{8\pi}\int_V \boldsymbol{H}^2\,\mathrm{d}\boldsymbol{r} = 2tSw_d = 2tS\sum_{\boldsymbol{k}} w_{\boldsymbol{k}} \tag{13}$$

where S is the ferromagnetic film area, w_d is the effective average volume energy density, and $w_{\boldsymbol{k}}$ denotes the contribution related to the particular $\boldsymbol{k}$ vector.

For the analysis of static properties of domain structures in thin films we may neglect terms proportional to $\boldsymbol{k}\cdot\boldsymbol{M}_{\boldsymbol{k}}$. Then the last formula can be written in the simpler form

$$w_{\boldsymbol{k}} = 2\pi|M_{\boldsymbol{k}}^{z}|^2[1 - f(kt, \lambda_+/t, \lambda_-/t)] = 2\pi|M_{\boldsymbol{k}}^{z}|^2 + \tilde{w}_{\boldsymbol{k}}. \tag{14}$$

We see that the first term in the above expression can be included in the energy of the uniaxial anisotropy. This term is independent of superconductor parameters and remains the characteristic feature of any ultra-thin film [5]. The effective anisotropy constant is given by

$$\tilde{K}_u = K_u - 4\pi M_0^2. \tag{15}$$

Then $\tilde{w}_{\boldsymbol{k}}$ plays the role of the effective demagnetization energy, related to the non-uniformity of magnetization distribution.

In order to simplify notation, we will use new variables $\nu = kt$ and $\Lambda = \lambda_+/t$. The parameters $\kappa_\pm$ have been defined already (10). For the particular cases mentioned above, the f function has the following forms.

2.4.1. The symmetric configuration ($\lambda_+ = \lambda_- = \Lambda t$).

$$f(\nu, \Lambda, \Lambda) = \{1 - [1/(2\nu) - \kappa_+]\sinh(2\nu) + [1 - \kappa_+/(2\nu)](1 + \kappa_+^2)\sinh^2\nu\}/(\cosh\nu + \kappa_+\sinh\nu)^2 \tag{16}$$

where, according to (10), $\kappa_+ = k/k_+ = [1 + (\Lambda\nu)^{-2}]^{-1/2}$.

For an ideal superconductor ($\lambda_+ \to 0$) we obtain

$$f(\nu, 0, 0) = 1 - (\tanh\nu)/\nu. \tag{17}$$

2.4.2. Non-superconducting cover ($\lambda_- - \infty$).

$$f(\nu, \Lambda, \infty) = 1 - \frac{1 - e^{-4\nu}}{4\nu} - \frac{\kappa_+^2 - \kappa_+ + 2}{\kappa_+ + 1}\frac{(1 - e^{-2\nu})^2}{4\nu}. \tag{18}$$

Now, in the limit of ideal superconducting substrate ($\lambda_+ \to 0$) we obtain

$$f(\nu, 0, \infty) = 1 - [1 = e^{-4\nu} + 2(1 - e^{-2\nu})^2]/4\nu. \tag{19}$$

In the limit of $\lambda_+ \to \infty$ this corresponds to the situation of non-superconducting substrate and capping, leading to the well known formula (see e.g. [4])

$$f(\nu, \infty, \infty) = 1 - (1 - e^{-2\nu})/2\nu. \tag{20}$$

3. Stripe domain structure

Let us consider a simple, one-dimensional model of domain structure, composed of uniformly magnetized stripes of width L. The magnetization is aligned alternately in the $\pm z$-directions, and sharp domain boundaries are parallel to the yz-plane. Such a model is well justified at relatively high anisotropy (i.e. large quality factor). It was investigated previously in [4] for an ultra-thin film deposited on normal substrate.

The distribution of the magnetization vector can be expressed as

$$\boldsymbol{M} = M_0\left(0, 0, \sum_{\substack{n=1\\ odd}}^{\infty}\frac{4\sin(k_n x)}{\pi n}\right) \qquad k_n = \frac{\pi n}{L}. \tag{21}$$

This corresponds to

$$M_{\boldsymbol{k}}^z = M_0\delta(k_y)\sum_{\substack{n=1\\ odd}}^{\infty}\frac{2i}{\pi n}[\delta(k_x + k_n) - \delta(k_x - k_n)] \tag{22}$$

where

$$\delta(k) = \begin{cases} 1 & \text{for } k = 0 \\ 0 & \text{for } k \neq 0. \end{cases}$$

The averaged energy, per unit volume of the film, arising from domain walls is given by

$$w_w = \sigma_0/L \tag{23}$$

where $\sigma_0 = 4\sqrt{A\tilde{K}_u}$ is the surface energy of the wall. Here A denotes the stiffness constant.

The equilibrium domain size can be found by minimization of the sum $w_d + w_w$, which is equivalent to

$$\frac{l_h}{L} - \sum_{\substack{n=1\\ odd}}^{\infty} \left(\frac{2}{\pi n}\right) f\left(\pi n \frac{t}{L}, \Lambda_+, \Lambda_-\right) = \min \tag{24}$$

where $l_h = \sigma_0/4\pi M_0^2$ is the characteristic length.

In general, this sum must be analysed numerically. The curves $L(t)$ corresponding to different penetration depths are shown in figure 2. For thick films ($t \gg L$), the domain size in the free film is larger than in films deposited on a superconductor. In this case, the field of the superconducting currents adds to the self-demagnetizing field inside the ferromagnet, increasing the near-zone dipolar energy. On the other hand, for thin films ($t \ll L$) the domain size in the free film becomes smaller than in the case of a superconducting substrate. This can be understood taking into account the change of the far-zone demagnetizing field characteristic (see figure 1). The increase is much faster for smaller penetration depth. Since the multipolar terms decrease with distance much faster than the dipolar one, a critical thickness exists, where the monodomain state becomes the most efficient energetically ($L \to \infty$). This argument remains in agreement with results obtained in [3], where the authors, using a very approximation of the demagnetizing energy, showed that the second-order phase transition induced by an in-plane field can produce a uniform canted phase (i.e. $L = \infty$) rather than domain structure. There was also a suggestion, supported by numerical calculations, that the monodomain state has the minimal energy even in a zero in-plane field. We will deal with this problem in the next sections.

On the other hand, the problem is easily solveable at large thickness for ideal superconductors. Let us note, again, that we assume large uniaxial anisotropy. For $\lambda_\pm \to \infty$ we have $\kappa_\pm \to 1$, which gives the sum analysed in [4]. In the case of a thick film ($t \gg L$) we can additionally put $kt \gg 1$ and obtain the well known formula for equilibrium domain size [6]:

$$\begin{cases} f(\nu, \infty, \infty) \approx 1 - 1/2\nu \\ L_\infty = 2\pi\sqrt{\pi l_h t/7\zeta(3)} \end{cases} \tag{25}$$

where $\zeta(3)$ is the Riemann zeta function.

3.1. The symmetric configuration ($\lambda_+ = \lambda_-$)

For $\lambda_+ \to 0$ we have $\kappa_+ \to 0$ and in the thick-film limit the effective demagnetization energy is changed by a factor of two at most. This leads to the result

$$\begin{cases} f(\nu, 0, 0) \approx 1 - 1/\nu \\ L_s(\lambda_+ = 0) = L_\infty/\sqrt{2}. \end{cases} \tag{26}$$

Let us note that the factor by which the domain size changes is not directly dependent on L_∞.

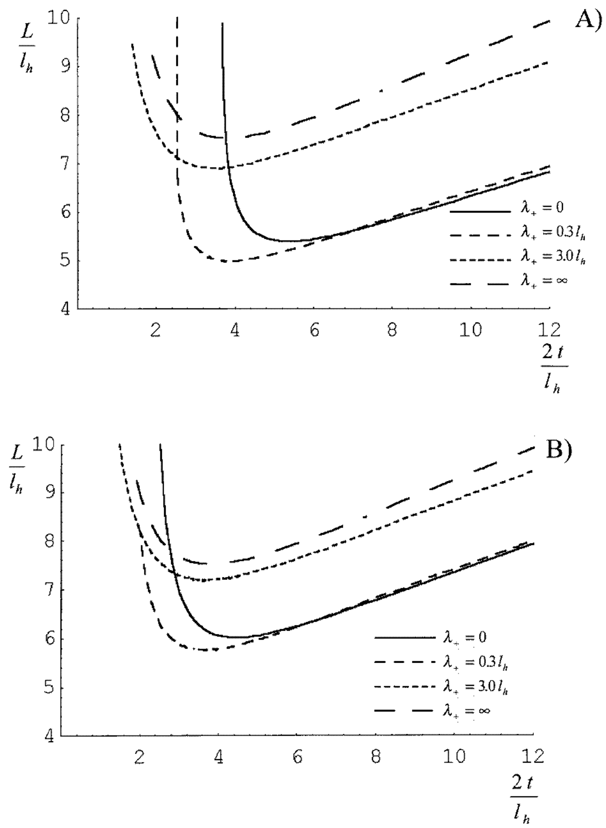

Figure 2. Equilibrium domain size $L(t)$ dependences, corresponding to different penetration depths, for (A) the symmetric case and (B) vacuum capping. $2t$ is the ferromagnetic film thickness.

3.2. Non-superconducting cover ($\lambda_- = \infty$)

This case is especially important, since it seems that such films may be much easier to fabricate and to observe. However, there is no qualitative difference from the case discussed above. The L_∞ value certainly remains the same, and $\lambda_+ \to 0$ changes the effective demagnetization term by a factor of 3/2. Hence

$$\begin{cases} f(\nu, 0, \infty) \approx 1 - 3/4\nu \\ L_n(\lambda_+ = 0) = L_\infty/\sqrt{3/2}. \end{cases} \tag{27}$$

4. Critical thickness: an isolated Bloch domain wall

As was shown before, in ultra-thin films deposited on a superconductor the equilibrium domain size quickly increases as the thickness decreases; this is related to the local character of the demagnetization forces. It was also supposed that there are critical values $t_c(\lambda)$, corresponding to domain structure suppression. The energy of the domain wall is always positive (as compared with the uniform state), and for domain structure creation it is necessary to compensate it with a negative demagnetization energy contribution (in our case the uniform part of the demagnetization energy has re-normalized the anisotropy constant). When the domain size tends to infinity such energy energy balance can be performed for each wall separately, and the critical thickness for domain suppression can be assigned to a t_c value, at which this balance becomes less profitable than in the monodomain state. We shall consider a one-dimensional Bloch wall centred on the plane $x = 0$. We assume the magnetization distribution in the standard form:

$$\boldsymbol{M} = M_0(0, \sin\theta, \cos\theta) \qquad \sin\theta = 1/\cosh(x/\Delta) \tag{28}$$

where Δ is the wall width. Its value is a function of exchange and anisotropy constants, as well as thickness for ultra-thin films. Then the only non-vanishing Fourier components can be written as

$$\begin{cases} M^y_{k_x} = m^y_k M_0 = \dfrac{\pi\Delta}{\cosh(\pi k\Delta/2)} M_0 \\ M^z_{k_x} = m^z_k M_0 = -\dfrac{\pi \mathrm{i}\Delta}{\sinh(\pi k\Delta/2)} M_0. \end{cases} \tag{29}$$

In order to investigate the balance of energy, we can consider linear energy density ε (per unit length of the wall), normalized by M_0^2. We will take into account the following energy contributions.

(i) *Exchange energy.*

$$\varepsilon^{ex}_k = \tfrac{1}{2} a k^2 (|m^y_k|^2 + |m^z_k|^2) = 2\pi^2 \alpha k^2 \Delta^2 \cosh(\pi k\Delta)/\sinh^2(\pi k\Delta) \tag{30}$$

where $\alpha - 2A/M_0^2$.

(ii) *Anisotropy energy (including the uniform part of demagnetization).*

$$\varepsilon^{an}_k = \tfrac{1}{2}(\beta - 4\pi)|m^y_k|^2 = \pi^2\tilde{\beta}\Delta^2/2\cosh h^2(\pi k\Delta/2) \tag{31}$$

where $\beta = 2K_u/M_0^2$ and $\tilde{\beta} = \beta - 4\pi$.

Exchange and anisotropy contributions are positive and can be written together as

$$\varepsilon_> = \frac{I}{\pi}\int_0^\infty (\varepsilon^{ex}_k + \varepsilon^{an}_k)\,\mathrm{d}k = \frac{\alpha}{\Delta} + \tilde{\beta}\Delta. \tag{32}$$

(iii) *Non-uniform demagnetizing energy.* This contribution is negative and has the form

$$\varepsilon_< = -2\int_0^\infty |m^z_k|^2 f(kt, \Lambda_+, \Lambda_-)\,\mathrm{d}k = -8t\rho^2 J(\rho, \Lambda_+, \Lambda_-) \tag{33}$$

where $\rho = \pi\Delta/2t$ and $J(\rho, \Lambda_+, \Lambda_-) = \int_0^\infty \mathrm{d}\nu f(\nu, \Lambda_+, \Lambda_-)/\sinh^2(\rho\nu)]$.

The total energy of the isolated Bloch wall is given by

$$\varepsilon = \varepsilon_> + \varepsilon_< = \alpha/\Delta + \tilde{\beta}\Delta - 8t\rho^2 J(\rho, \Lambda_+, \Lambda_-). \tag{34}$$

Δ can be evaluated by minimization of the energy ε. Simultaneously, for the critical thickness this energy has to be equal to the energy of the uniform phase (i.e. zero). Hence we obtain the set of two non-linear equations defining critical values of the parameters t and ρ.

$$\begin{cases} \tilde{\beta} = 6\pi\rho J(\rho, \Lambda_+, \Lambda_-) + 2\pi\rho^2 J'_\rho(\rho, \Lambda_+, \Lambda_-) \\ \pi\alpha/4t^2 = -4\pi\rho^3 J(\rho, \Lambda_+, \Lambda_-) - 4\pi\rho^4 J'_\rho(\rho, \Lambda_+, \Lambda_-). \end{cases} \tag{35}$$

In general the above equations can be solved numerically for $\tilde{\beta} > 0$. The dependences $2t_c(Q > 1)$ are presented in figure 3, where $Q = \beta/(4\pi)$ is the quality factor of the

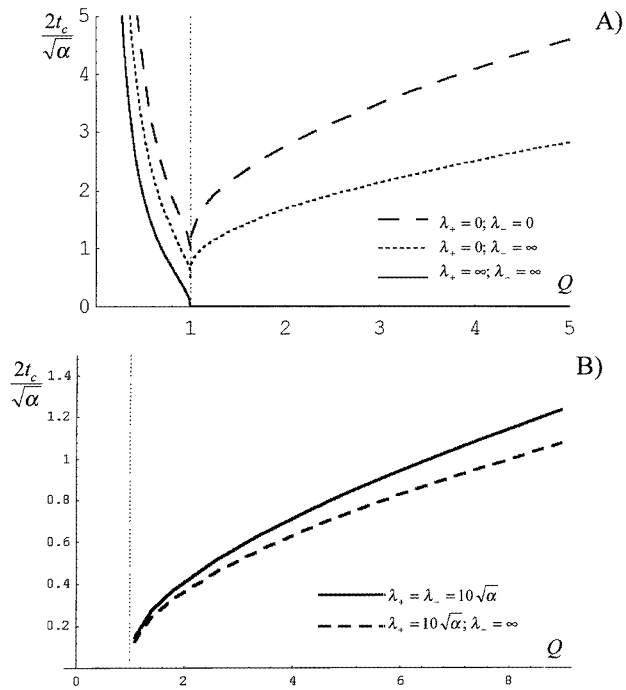

Figure 3. Critical thickness $t_c(Q)$ dependences for (A) an ideal superconductor and (B) finite penetration depth, calculated for different substrate–capping combinations. Q is the quality factor of the ferromagnetic material.

ferromagnet. Figure 3(B) corresponds to a realistic value of $\lambda_+ = 10\sqrt{\alpha}$. It can be seen for large Q-values the critical thickness is of order $\sqrt{\alpha}$. As an example, for hcp cobalt $\sqrt{\alpha} \approx 110$ Å, and we have $t_c(\lambda_+ = 1100\ \text{Å}) \propto 110$ Å. The t_c-values for the symmetric case and non-superconducting capping are of the same order.

Figure 4 shows $2t_c(\lambda_+)$ curves for different anisotropy values. After the fast drop in the region of small penetration depth, $2t_c$ decreases very slowly (logarithmically) with increasing λ_+. Let us remark that the critical thickness remains significant (tens of ångströms) independently of the capping type, even for large λ_+ and small anisotropy.

For vacuum surrounding we obtain $\lim_{\lambda_x \to \infty} t_c = 0$, i.e. the monodomain state is unstable at any finite thickness.

Let us consider the case of an ideal superconductor ($\lambda_+ = 0$).

4.1. The symmetric configuration ($\lambda_- = \lambda_+$)

4.1.1. Large anisotropy ($\rho \ll 1$).

$$J(\rho, 0, 0) \approx \frac{1}{2\rho^2} \int_0^\infty \frac{\mathrm{d}\nu \tanh^2 \nu}{\nu^2} \approx \frac{0.8525}{\rho^2} \tag{36}$$

$$\Delta_c \approx \sqrt{\alpha/\tilde{\beta}} \qquad 2t_c \approx 0.5865\sqrt{\alpha\tilde{\beta}}. \tag{37}$$

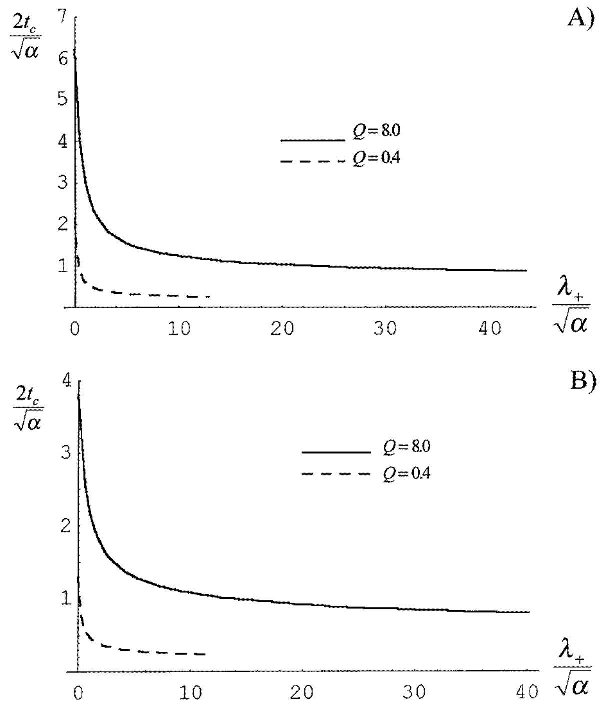

Figure 4. Critical thickness $t_c(\lambda_+)$ dependences for (A) the symmetric case $\lambda_- = \lambda_+$ and (B) vacuum capping $\lambda_- = \infty$, calculated for different quality factors Q.

4.1.2. Small anisotropy ($\rho \gg 1$).

$$J(\rho, 0, 0) \approx \int_0^\infty \frac{d\nu}{\sinh^2(\rho\nu)} \left(\frac{1}{3}\nu^2 - \frac{2}{15}\nu^4\right) \approx \frac{\pi^2}{18\rho^3} - \frac{\pi^4}{225\rho^5} \tag{38}$$

$$\Delta_c \approx (9\alpha^2/25\pi\tilde{\beta})^{1/4} \qquad 2t_c \approx 3\sqrt{\alpha/2\pi}. \tag{39}$$

4.2. Non-superconducting cover ($\lambda_- = \infty$)

4.2.1. Large anisotropy ($\rho \ll 1$).

$$J(\rho, 0, \infty) \approx (2\ln 2)/\rho^2 \approx 1.3863/\rho^2 \tag{40}$$

$$\Delta_c \approx \sqrt{\alpha/\tilde{\beta}} \qquad 2t_c \approx \sqrt{\alpha\tilde{\beta}/4\ln 2} \approx 0.3607\sqrt{\alpha\tilde{\beta}}. \tag{41}$$

4.2.2. Small anisotropy ($\rho \gg 1$).

$$J(\rho, 0, \infty) \approx \int_0^\infty \frac{d\nu}{\sinh^2(\rho\nu)} \left(\frac{4}{3}\nu^2 - 2\nu^3\right) \approx \frac{2\pi^2}{9\rho^3} - \frac{3\zeta(3)}{\rho^4} \tag{42}$$

$$\Delta_c \approx (3/2\pi)(6\pi\zeta(3)/\tilde{\beta})^{1/3}\sqrt{\alpha/2\pi} \qquad 2t_c \approx \tfrac{3}{2}\sqrt{\alpha/2\pi}. \tag{43}$$

5. Critical thickness: sinusoidal domain structure

As shown in [7], for $0 < \beta < 4\pi$ (which corresponds to the effective in-plane anisotropy) the amplitude of domain structure is lower than M_0 and tends to zero ($|m_k^2| \ll 1$) when

$t \to t_c + 0$. At the same time, the domain size tends to the finite value L_c, and $\Delta/L_c \to 1$. This means that the critical domain structure has sinusoidal shape and its energy can be expressed as

$$\varepsilon = \varepsilon_k = [\tfrac{1}{2}\alpha k^2 - \tfrac{1}{2}\tilde{\beta} - 2\pi f(kt, \Lambda_+, \Lambda_-)]|m_k^z|^2 + \mathrm{O}(|m_k^z|^4). \tag{44}$$

At the point of phase transition the expression in the square brackets is equal to zero, and the energy should achieve a minimum as a function of k. These conditions give the following equation set, defining t_c and k_c:

$$\begin{cases} Q = 1 + \tfrac{1}{2}\nu f'_\nu(\nu, \Lambda_+, \Lambda_-) - f(\nu, \Lambda_+, \Lambda_-) \\ \alpha/4\pi t^2 - f'_\nu(\nu, \Lambda_+, \Lambda_-)/2\nu \end{cases} \tag{45}$$

where $\nu = kt$. The numerical solution of (45) is shown in figure 4 as curves corresponding to $Q < 1$.

5.1. *The symmetric configuration ($\lambda_- = \lambda_+$)*

In this case of $Q \to 1$ from below we obtain $L_c \to \infty$ and

$$2t_c \to -\tfrac{9}{2}\lambda_+ + \sqrt{\tfrac{81}{4}\lambda_+^2 + 3\alpha/\pi}. \tag{46}$$

5.2. *Non-superconducting cover ($\lambda_- = \infty$)*

For $Q \to 1$ from below we have again $L_c \to \infty$ and

$$2t_c \to -\tfrac{1}{2}\left(-\tfrac{9}{2}\lambda_+ + \sqrt{\tfrac{81}{4}\lambda_+^2 + 3\alpha/\pi}\right). \tag{47}$$

5.3. *Vacuum surroundings ($\lambda_\pm = \infty$)*

For $1 - Q \ll 1$ we obtain

$$\begin{cases} 2t_c \approx 2\sqrt{(\alpha/\pi)(1-Q)} \\ L_c \approx \tfrac{1}{2}\sqrt{\pi\alpha/(1-Q)}. \end{cases} \tag{48}$$

For $Q \ll 1$ the behaviour is independent of $\lambda_\pm$:

$$\begin{cases} 2t_c \approx \tfrac{3}{4}\sqrt{\pi\alpha/Q^3} \\ L_c \approx \tfrac{1}{2}\sqrt{3\pi\alpha/Q}. \end{cases} \tag{49}$$

For any finite $\lambda_\pm$ the dependence $t_c(Q)$ has a discontinuity at $Q = 1$, which is related to the different character of the phase transitions.

6. Conclusion

We have shown that superconducting surroundings significantly affect parameters of domain structures in ferromagnetic films, both in ultra-thin and thick limits. This leads to the full suppression of domain structure when the film thickness is lower than a critical value t_c, which is a function of London penetration depth and parameters of the ferromagnet. However, for practically expected values of these factors, it remains not small (tens of ångströms), even for non-superconducting capping.

In the above analysis, we assumed that equilibrium domain structure is defined exclusively by phenomenological interactions typical for ideal materials, neglecting any influence of defects. In fact, very often ultra-thin films contain numerous defects, which can strongly affect the domain structure creation. This effect may completely suppress the magnetostatic interactions between ferromagnet and superconductor.

On the other hand, there is an open problem of the superconductor influence on magnetic properties of ultra-thin films, which was neglected in our consideration. There may be an effect of Cooper pair tunnelling into the ferromagnetic metallic film that can significantly change both exchange and anisotropy constants. This can lead to creation of different kinds of inhomogeneous magnetic moment distribution [8]. We have also neglected the possible suppression of the superconducting order parameter near the ferromagnet–superconductor interface, due to the strong exchange field of the ferromagnetic film [8, 9]. In fact, both mechanisms mentioned may create a 'dead' layer between ferromagnet and superconductor, which is neither ferromagnet nor superconducting.

Finally, we assumed that the anisotropy constant and the film thickness are independent parameters. It is known that in the ultra-thin limit they are closely connected, which should be taken into account in calculations made for real films.

Acknowledgments

The authors are indebted to Professor A S Kovalev, Professor A S Sukstansky and S V Tarasenko for helpful discussions. One of us (AS) gratefully acknowledges the hospitality of the University of Sheffield.

The work was supported by HCM network No CHRX-CT93-0316.

References

[1] Bland J A C and Heinrich B (ed) 1994 *Ultra Thin Magnetic Structures* (Berlin: Springer)

[2] Bespyatkh Yu I, Wasilewski W, Gajdek M, Simonov A D and Kharitonov V D 1994 Suppression of magnetic domains in layered ferromagnetic-type-II-superconductor structures *Fiz. Tverd. Tela* **36** 586 (Engl. transl. *Sov. Phys.–Solid State* **36** 323)

[3] Sadreev A F 1993 Influence of superconducting substrates on the domain structure of a magnetic film with a uniaxial anisotropy *Fiz. Tverd. Tela* **35** 2099 (Engl. transl. *Sov. Phys.–Solid State* **35** 1044)

[4] Kaplan B and Gehring G A 1993 The domain structure of ultra thin magnetic film *J. Magn. Magn. Mater.* **128** 111

[5] Stankiewicz A, Tarasenko S V, Tarasenko V V and Ferre J unpublished

[6] Landau L D and Lifshitz E M 1984 *Electrodynamics of Continuous Media* (Oxford: Pergamon)

[7] Baryakhtar V G and Ivanov B A 1977 Phase diagram of a ferromagnetic plate in an external magnetic field *Zh. Eksp. Teor. Fiz.* **72** 1504 (Engl. transl. *Sov. Phys.–JETP* **45** 789)

[8] Buzdin A I and Bulaevsky L N 1988 Ferromagnetic film on the surface of a superconductor: possible onset of inhomogeneous magnetic ordering *Zh. Eksp. Teor. Fiz.* **94** 256 (Engl. transl. *Sov. Phys.–JETP* **67** 276)

[9] Koorevaar P, Coehoorn R and Aarts J 1995 Critical fields in vanadium-based superconducting/ferromagnetic multilayers *Physica* C **248** 61